

ZBLLAC: A spectroscopic database of BL Lacertae objects.

MARCO LANDONI  ^{1,2} R. FALOMO  ³ S. PAIANO  ^{4,5} AND A. TREVES^{6,2}

¹ INAF - Istituto Nazionale di Astrofisica. Osservatorio Astronomico di Cagliari. Via della Scienza 5, 09047 Selargius (CA) - ITA

² INAF - Istituto Nazionale di Astrofisica. Osservatorio Astronomico di Brera Via E. Bianchi 46 - 23807 Merate (LC), ITA

³ INAF - Istituto Nazionale di Astrofisica. Osservatorio Astronomico di Padova, Vicolo Osservatorio 5 - 35122 Padova, ITA

⁴ INAF - Osservatorio Astronomico di Roma, via Frascati 33, I-00040, Monteporzio Catone, Italy

⁵ INAF - Istituto Nazionale di Astrofisica. IASF Istituto di Astrofisica e Fisica Cosmica, Via Alfonso Corti 12 - 20133 Milano, ITA

⁶ Universit degli Studi dell' Insubria Via Valleggio 11, 22100 Como, ITA

(Received July 20, 2020)

ABSTRACT

This paper describes the database of optical spectra of BL Lacertae (BLL) objects ZBLLAC available at the URL <https://web.oapd.inaf.it/zbllac/>. At the present date, it contains calibrated spectra for 295 BLL. For about 35% of them, we report a firm measure of redshift z while for 35 sources we set a lower limit on z based on the detection of intervening absorption systems, mainly ascribed to Mg II (λ 2800 Å). We report here on the architecture of the database and on its web front-end that permits to filter, query and interactively explore the data. We discuss some properties of the objects in the present dataset by giving the distribution of the redshifts and reporting on the detected emission lines, which turn out to be mainly forbidden and ascribed to [O II] (λ 3737 Å) and [O III] (λ 5007 Å). Finally, we discuss on intervening absorption systems detected in 35 BLLs that allow us to set lower limits to their distance.

1. INTRODUCTION

BL Lacertae (BLL) are a peculiar class of low power ($L \sim 10^{43}$ erg sec $^{-1}$) Active Galactic Nuclei (AGN) whose relativistic jet, generated by the accretion of matter onto a supermassive black hole, is closely aligned with the observer's line of sight (e.g. Blandford & Rees 1978). In this condition, the radiation produced by the jet is boosted due to the relativistic Doppler aberration, and in most cases dominates the Spectral Energy Distribution (SED) at almost any wavelength of the electromagnetic spectrum (see e.g. Maraschi et al. (1992); Ghisellini et al. (1993); Urry & Padovani (1995)). A peculiar spectroscopic characteristic of BLL is that, at variance with other active galactic nuclei, the emission lines are absent or extremely weak (see e.g. Falomo et al. (2014) for a recent review) and the boosted non-thermal continuum, in most of the cases, outshines the contribution from the starlight of the host galaxy, which is typically a giant Elliptical with $M_v \sim -22.50$ (Sbarufatti et al. 2005a). More generally, BLL are a subclass of a larger parent population called Blazars, which encom-

pass also more powerful sources (namely Flat Spectrum Radio Quasars, FSRQ) with bolometric luminosity of the order of 10^{47} , 10^{48} erg sec $^{-1}$ and optical spectra characterized by broad emission lines typical of quasars, suggesting the presence of a radiatively efficient accretion disk (Shakura & Sunyaev 1973).

The quasi-featureless continuum exhibited by BL Lacs is a characteristic that made them rather elusive since the determination of the redshift, which is a fundamental parameter to determine the distance and derive physical quantities, is in many cases hindered. Historically, various groups made huge efforts to secure spectroscopic data with small-medium sized telescopes aiming to increase the number of BLL for which a firm determination of z was assessed, although for many objects this was limited to bright or moderately beamed sources due to the modest signal-to-noise ratio reachable with the available instrumentation (e.g. Miller et al. (1978); Stickel et al. (1988, 1989); Falomo & Treves (1990); Falomo et al. (2002)).

Many surveys from radio band (e.g. 1 Jy radio catalog, Stickel et al. (1991)) to X-Ray missions (for instance the Einstein Observatory, ROSAT) allowed to increase the sample of known candidate BLLs stimulating spectroscopical follow ups in the optical band, that

were carried out with various optical telescope facilities (see e.g. Stocke et al. (1985); Lawrence et al. (1996) and reference therein). The availability of deep optical surveys like the Sloan Digital Sky Survey (SDSS) also contributed to enlarge the number of BLLs. In particular, Plotkin et al. (2010) by combining data from SDSS and radio catalogs discovered about 700 BLLs candidates and constrained the z for 30% of them. More recently at high energies, the advent of FERMI mission (Atwood et al. 2009) showed that BLLs represent the dominant extragalactic population in gamma-rays and, intriguingly, that for most of them only poor quality spectroscopical data were available. Various methodologies, based on multi wavelength data (e.g. Massaro et al. (2011, 2012b, 2013); Nori et al. (2014); Massaro et al. (2014); D'Abrusco et al. (2014); Massaro et al. (2015c, 2016); Massaro & D'Abrusco (2016); Paiano et al. (2017a) and reference therein), developed to associate low-energy counterparts of objects detected by FERMI further encouraged spectroscopic campaigns (e.g. Paggi et al. (2014); Landoni et al. (2015a); Massaro et al. (2015b); Ricci et al. (2015); Álvarez Crespo et al. (2016a,b,c); Paiano et al. (2017b); Marchesi et al. (2018); Peña-Herazo et al. (2019)). In this context, hundreds of BLLs spectra have been successfully secured (see e.g. the review from Massaro et al. (2016)) but only for the brightest targets the redshift was measured. In fact, for the faintest sources or extremely beamed BLLs, only observations with large aperture optical telescope (like the Very Large Telescope, Keck Telescope and Gran Telescopio CANARIAS) equipped with state-of-the-art instrumentation could allow to secure high signal-to-noise ratio spectra of these targets and reveal weak spectral features (intrinsic or intervening) to firmly determine their redshift (see e.g. Sbarufatti et al. (2005b, 2006, 2009); Landoni et al. (2013); Sandrinelli et al. (2013); Landoni et al. (2015a,b, 2018); Shaw et al. (2013); Pita et al. (2014); Paiano et al. (2017b,c, 2018, 2019)).

The results of all these spectroscopic campaigns are frequently summarised across multi-wavelength catalogues in the literature (e.g. Roma BZCat, TevCAT see Wakely & Horan (2008); Massaro et al. (2015a)) but none of them allows scientists to access the fully calibrated spectra of the sources with a homogeneous set of figures that permit to identify the spectral features detected in the spectra and then reuse the data for many different scientific aims. Motivated by these facts, we developed a new web-based database of BL Lac objects, namely ZBLLAC (<https://web.oapd.inaf.it/zblac/>), able to act as an online hub where optical spectra secured in the context of different publications with heterogeneous instru-

mentation are stored and made available to the community.

We present in this paper the properties of the database and of the web application. ZBLLAC includes a smart representation of the data to provide a facilitated access to the basic information of each source and, specifically, to the machine readable 1-D calibrated spectra along with a PDF figure that shows the spectroscopic identification of firmly detected emission or absorption lines. The paper is organized as follows: in Section 2 we give an overview of our database and the website while in Section 3 we detail on the format of our data. In Section 4 we discuss properties of the dataset and we report our conclusions and future perspectives in Section 5.

2. THE ZBLLAC SPECTROSCOPIC DATABASE

At the time of writing of this work, the ZBLLAC database contains 337 objects considered as BLL or BLL candidates in the literature. The sources were selected among heterogeneous criteria such as their detection in γ -rays at GeV or TeV band (see e.g. Atwood et al. (2009); Paiano et al. (2017b), WISE infrared colour (Massaro et al. (2012a); D'Abrusco et al. (2019); de Menezes et al. (2019, 2020)) or the properties of their broadband SED (Padovani & Giommi (1995a,b); Costamante & Ghisellini (2002); Costamante (2020)). According to the properties of their optical spectra in ZBLLAC, we labeled 295 objects as BLL by adopting spectral criteria based on the absence of emission features or, if detected, on the value of the EW, luminosities and broadness of the lines. The remaining 42 targets exhibit spectra dominated by broad and intense emission lines, suggesting to us an alternative classification and for this reason they have not been considered as BLL.

For each object we give α , δ , catalog name, redshift, magnitude and provide a flux calibrated spectrum¹, dereddened for Galactic extinction. The spectra are available both in text format and with a PDF figure which reports both the flux calibrated and normalized spectra. The main detected features, if present, are marked and identified (see examples of Figure 1). We also note that for 37 BLLs more than one spectrum, secured in different epochs and with different instrumentation, is reported in the database.

The web interface of ZBLLAC is reported in Figure 2. The user can retrieve and interactively explore the data through the Spectroscopic Database page, that shows by default the full list of sources present in ZBLLAC.

¹ Data were made available to us in electronic form directly from the Authors. For further details see <https://web.oapd.inaf.it/zblac/refindex.html>

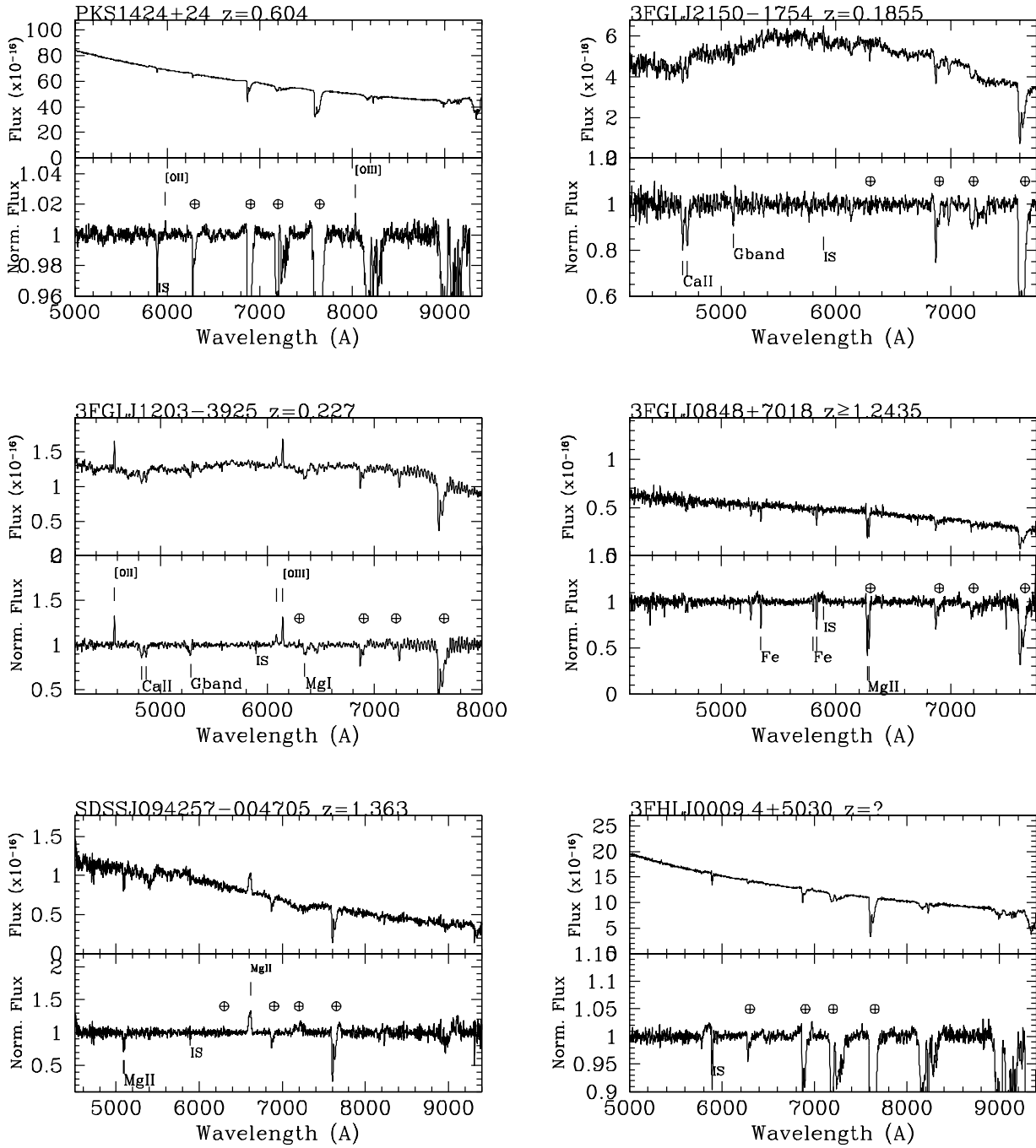


Figure 1. Examples of spectra contained in the ZBLLAC database. PKS1424+24: redshift derived from weak forbidden lines ascribed to [O II] and [O III] (Paiano et al. 2017c). 3FGL J2150–1754: The z follows from absorption lines ascribed to the host galaxy (Paiano et al. 2017b). 3FGL J1203–3925: The redshift derives from emission lines and features from the host galaxy (Peña-Herazo et al. 2017; Marchesini et al. 2019). 3FGL J0848+7018: The only apparent lines are due to intervening Mg II and Fe absorption systems, which yields a lower limit to the redshift (Paiano et al. 2017b). SDSS J0942257–004705: The redshift is constrained through emission line from Mg II and absorption line from intervening system (Landoni et al. 2018). 3FHL J0009.4+5030: The continuum is completely featureless and the redshift is unknown (Paiano et al. 2020).

For each of them, the application displays basic information and a set of buttons to download the spectrum and the annotated PDF figure. When more than one observation is associated to the same object, a further button is displayed allowing to select the spectrum, or figure, to download among all the available ones for the source. Finally, we implemented a Search Panel, shown on top of the page as reported in Figure 2, that permits to actively filter the database according to various criteria such as coordinate within a radius, target name or redshift range.

3. DATA FORMAT AND TECHNOLOGICAL ASPECTS

To store the data, we used the eXtensible Markup Language (XML²) standard that allows to define a proper data structure and model combining the possibility to easily query the database while being both machine and human readable. More specifically, the XML is a *markup language* that defines a set of rules for encoding plain-text documents in which the data are marked by tags or attributes (see Bosak & Bray (1999) for a full review). Data within XML documents are organized using a tree-like data structure, where each node may possess one or more leafs.

We decided to adopt a representation of the data by using the XML scheme reported in Figure 3. The root node of the structure is **zbl1ac** which contains, as leafs, the set of all objects of ZBLLAC database³. Each **object** (see Figure 3) contains as attributes all the relevant information to identify the source (name, coordinates, etc.) and two more nodes: the first one, named **nedlink**, contains the link to the object's NED page while the second (**spectra**) harbors a set of **spectrum** nodes where the information about each observation and the relative HTTP links to download the data are saved. To further illustrate the organisation of the data, we show in Figure 4 a sample node of our XML file for the object PKS 1553+113 for which three different spectra have been secured.

For what concerns the website backend, we made use of standard PHP pages coupled with XQuery and XPath⁴ protocols to retrieve the data throughout the XML file.

4. SPECTRAL PROPERTIES OF BLL

² <http://www.w3.org>.

³ The up-to-date version database can be download at this link : <https://web.oapd.inaf.it/zbl1ac/zbl1ac.xml>

⁴ ibm.com/developerworks/library/x-xpathphp/index.html

4.1. General properties

The dataset of BLL, that currently encompass 295 targets, can be retrieved using the Spectroscopic database page (see Figure 2) by selecting the flag **BLL**.

For 103 ($\sim 35\%$) objects intrinsic spectral features are revealed, allowing to firmly measure the redshift. In details, for 31 objects only emission lines are detected in their spectra while in 55 BLLs only features from the host galaxy (mainly ascribed to Ca II and G Band) are present. In 17 cases, both emission and absorption features are revealed on the same spectrum. The median value of z is 0.40, ranging between 0.071 and 1.636. The distribution of the redshifts is given in Figure 5 where we also report an histogram of z for objects in which the host galaxy has been detected. As shown in Figure 5, the determination of the redshift for object at $z \gtrsim 0.80$ is assessed only through emission lines since the features from host galaxy (e.g. Ca II $\lambda\lambda$ 3934-3968) start to move outside the covered spectral range (that for objects in ZBLLAC is, on average, between 4000 Å and 8000 Å).

Finally, for 35 BLLs that do not show intrinsic features we detected intervening absorption systems along the line of sight allowing to establish a firm lower limit to their redshift (see Section 4.3).

4.2. Emission lines properties

We detected emission features in 48 BLLs. The line identification and luminosities are given in Table 1.

In 28 cases, the only observed lines are narrow forbidden transition ascribed to [O II] (λ 3934 Å) and [O III] (λ 5007 Å) while broad spectral features, mainly associated to Mg II (λ 2800) and C III] (λ 1908), are revealed in just 8 targets. We also note that for only 4 cases broad and narrow emission lines are present on the very same spectrum. These facts may suggest that, in the majority of the cases, there is no trace of the broad line region possibly meaning that either the physical conditions for its appearance are absent, or that the lines are so broad and swamped by the continuum that they are not detected. We report in Figure 6 the distribution of the luminosity of emission lines ascribed to [O II] (λ 3934 Å) and [O III] (λ 5007 Å). The median luminosity for [O II] is 1.7×10^{41} erg s⁻¹ while in the case of [O III] we found 1.3×10^{41} erg s⁻¹.

Following the same approach described in Paiano et al. (2020), we compared our luminosities of [O II] and [O III] with those measured on spectra of low redshift QSOs (Shen et al. (2011), with similar luminosity on the continuum assuming a beaming factor $\delta \sim 10$) finding that their mean values are roughly similar. This result is in agreement with Paiano et al. (2020) but in this case our

The figure consists of two screenshots of a web browser displaying the ZBLLAC database. The top screenshot shows the homepage with a header featuring the ZBLLAC logo and a subtitle 'A SPECTROSCOPIC LIBRARY OF BL LAC OBJECTS'. Below the header are five navigation links: Home, Description of the library, The spectroscopic database, Contacts, and References. Two small astronomical images are visible on the left and right sides of the header. The main content area has a blue header bar with the text 'Optical spectra of BL Lac objects'. Below this, a text block describes the database, mentioning it contains optical spectra of ~300 BL Lac objects from various literature sources, with basic information like Name, Coordinates, Redshift, and Reference. The bottom screenshot shows a search panel with fields for Name, RA, DEC, Radius, Redshift range, and object type (BLL or QSO). Below the search panel is a table listing seven BL Lac objects with columns for Object name, RA (J2000), DEC (J2000), z, V, Setup, Spectrum, Type, and Reference. Each row includes a set of icons representing different types of spectra and data.

Object	RA (J2000)	DEC (J2000)	<i>z</i>	<i>V</i>	Setup	Spectrum	Type	Reference
ZBLL J0003+0841 (SDSSJ000359+084138)	00 03 59	+08 41 38	>1.5035	20.2	7		B	PAI17b
ZBLL J0006+0136 (SDSSJ000626+013610)	00 06 26	+01 36 10	0.787	20.3	7		B	PAI17b
ZBLL J0008+4712 (3FGL J0008.0+4713)	00 08 00	+47 12 08	>1.659	18.4	9		B	PAI17b
ZBLL J0015+5551 (3FGL J0015.7+5552)	00 15 40	+55 51 45	?	16.07	11		B	ALV16a
ZBLL J0022+0608 (PKS 0019+058)	00 22 32	+06 08 04	?	18.1	1		B	SBA09
ZBLL J0024-6820 (3FGL J0021.6-6835)	00 24 07	-68 20 55	0.354	15.7	10		FSRQ	MAR19
ZBLL J0031+0936 (SDSSJ003159+093618)	00 31 59	+09 36 18	0.2207	19.3	7		NLSy1	PAI17b

Figure 2. The ZBLLAC database web interface accessible at the link <https://web.oapd.inaf.it/zbllac/>. Upper panel: Home page of the website. Lower panel: A small portion of the spectral database page that shows the sources present in ZBLLAC and the Search Panel to select the objects on the basis of coordinates, redshift or literature name.

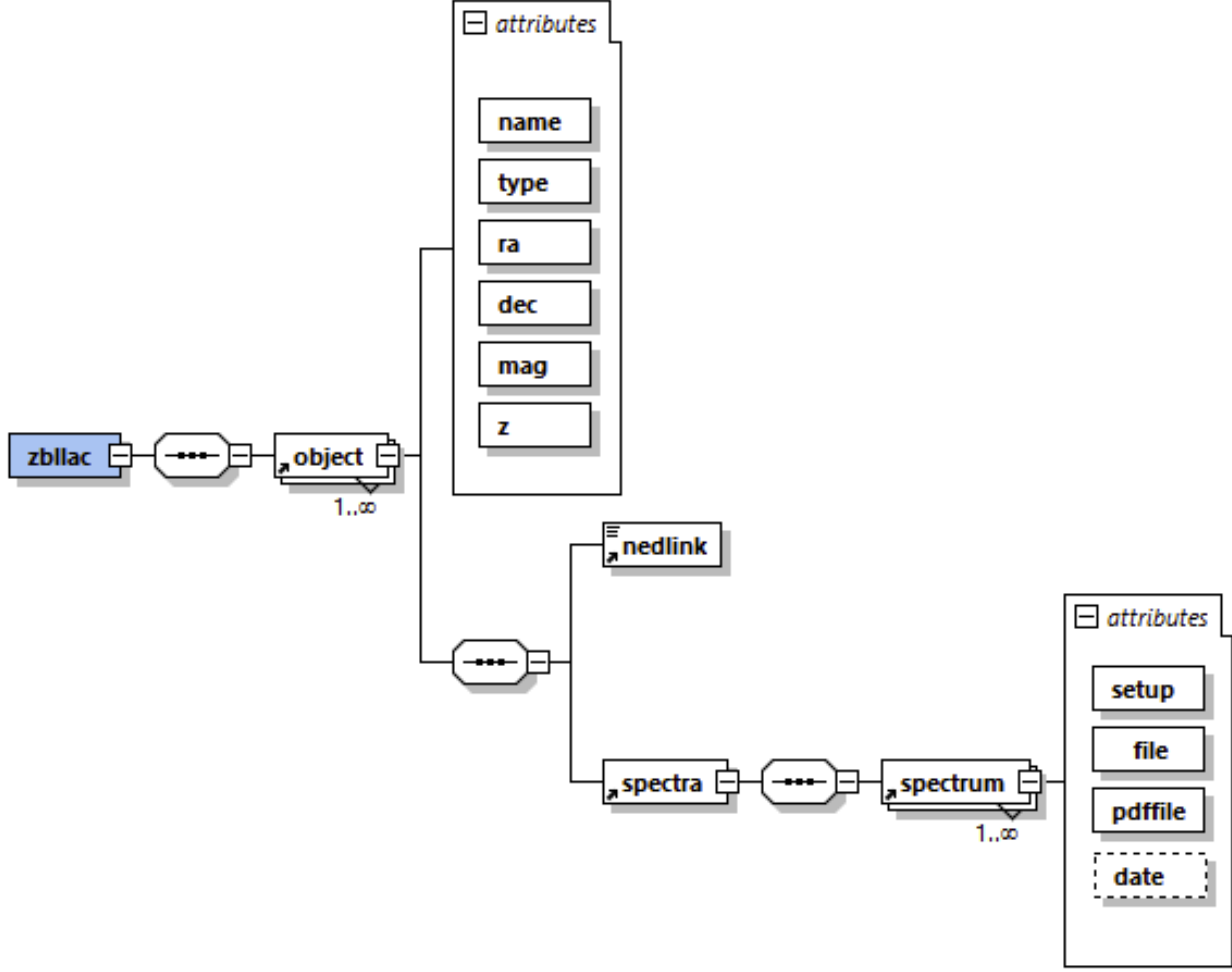


Figure 3. Schematic of the XML-based database adopted for the ZBLLAC database.

```

<object id="63" name="PKS 1553+113" type="B" ra="15 55 43" dec="+11 11 24" mag="14" z="?">
  <nedlink>
    <![CDATA[
      http://nedwww.ipac.caltech.edu/cgi-bin/nph-objsearch?objname=HB891553%2B113&extend=no&out_csys=Equatorial&out_equinox
    ]]>
  </nedlink>
  <spectra>
    <spectrum setup="1" spcfile="http://web.oapd.inaf.it/zbllac/txt/bl1553_vlt.txt"
      pdffile="http://web.oapd.inaf.it/zbllac/pdf/bl1553_vlt.pdf" ref="SBA06a"/>
    <spectrum setup="3" spcfile="http://web.oapd.inaf.it/zbllac/txt/bl1553_esob.txt"
      pdffile="http://web.oapd.inaf.it/zbllac/pdf/bl1553_esob.pdf" ref="Sbarufatti et al 2016" date="25 Jul 2001"/>
    <spectrum setup="6" spcfile="http://web.oapd.inaf.it/zbllac/txt/PG1553xsh.txt"
      pdffile="http://web.oapd.inaf.it/zbllac/pdf/bl1553xsh.zip" ref="Sbarufatti et al 2016" date="28 Apr 2010"/>
  </spectra>
</object>

```

ZBLL J1555+1111 (PKS 1553+113)	15 55 43	+11 11 24	?	14	1			B	SBA06a
--------------------------------	----------	-----------	---	----	---	--	--	---	--------

Figure 4. An example of the XML representation of the data for the object PKS 1553+113. For this source, three different spectra have been secured. The attributes `pdffile` and `spcfile` contain the full link on our website to download the figure and the 1-D calibrated spectra of the source. The lower blue panel shows how the row related to the source would be displayed on the ZBLLAC website.

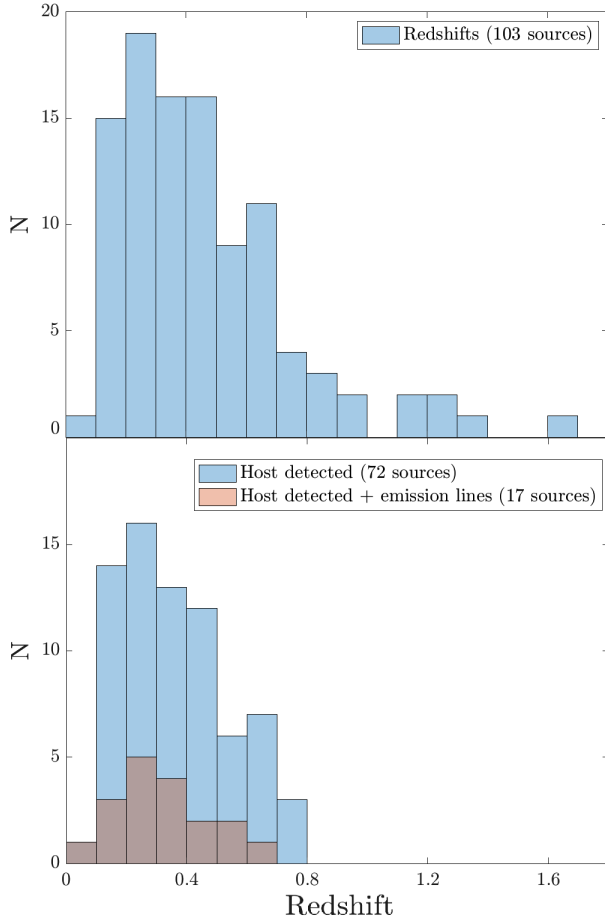


Figure 5. Distribution of the redshift of 103 BLL objects from the ZBLLAC database. Upper panel: distribution of z of the whole dataset. Lower panel (pale blue): redshift of the 72 sources in which the spectral features from the host galaxy have been detected. We report in shaded red the distribution of z for 17 BLLs in which both emission and absorption lines have been revealed.

conclusions are based on a dataset which is significantly larger.

4.3. Intervening absorption systems

In the spectra of BLLs, absorption lines could arise intrinsically from the host galaxy, yielding directly to the determination of z , or from intervening system if cool gases cloud structure is intercepted along the line of sight. In this case, the detection of an intervening absorption gives a robust lower limit to the redshift of the source. We detected those systems in 35 objects and we report our measurements on Table 2. In the wavelength range covered by our collection of spectra, the main absorption are those related to the Mg II doublet transition ($\lambda\lambda 2796-2803 \text{ \AA}$), when the redshift of the absorber is between $0.40 \leq z \leq 1.9$. In fact, in 30 cases we reveal spectral lines ascribed to Mg II ($\lambda 2800 \text{ \AA}$) that allow to

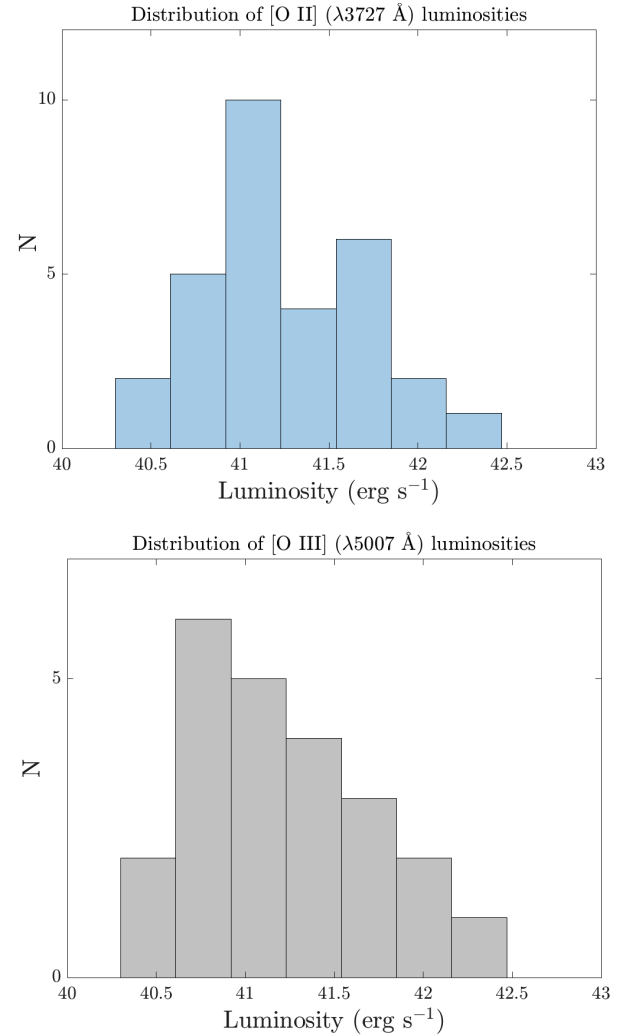


Figure 6. Distribution of the luminosity of emission lines from [O II] ($\lambda 3934 \text{ \AA}$) and [O III] ($\lambda 5007 \text{ \AA}$) detected in the spectra of BLLs in the ZBLLAC database.

set a lower limit to z . Furthermore, in three sources, both at redshift $z \gtrsim 2.00$, we detected the onset of Ly- α forest (see Landoni et al. (2018); Paiano et al. (2017b) for details) and further intervening system, at a lower redshift, associated to Mg II, C IV and Fe II (see Table 2). In a couple of targets, features arising from Ca II ($\lambda 3934 \text{ \AA}$) are detected in intervening systems along the line of sight.

The median value of our lower limits is $z \sim 0.64$ and we report in Figure 7 their distribution. The peak around $z \sim 0.60$ is related to our spectral range, where the probability of detection of Mg II is maximised. We note that lower limits for sources at $z \leq 0.40$ are in one case still ascribed to Mg II (ZBLL J0816–1311) because data has been obtained with ESO X-SHOOTER (Vernet et al. 2011) that provides increased spectral coverage in

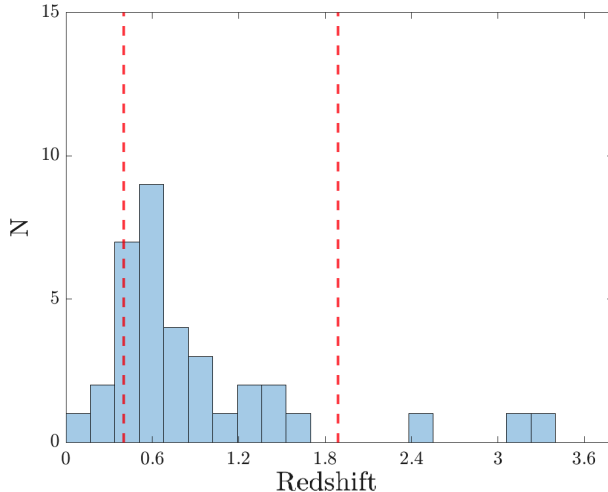


Figure 7. Distribution of the redshift lower limits of 35 BLLs. The two red vertical bars show the redshift range $0.35 \lesssim z \lesssim 1.90$ in which our spectral coverage allow to detect intervening absorption lines from Mg II.

the UV (Pita et al. 2014), while the other two cases are associated to intervening of Ca II ($\lambda 3934\text{\AA}$).

Finally, it is worthy to comment on the remaining 157 BLLs that still appear to be featureless. In our data, the total number of absorbers of Mg II, considering both multiple systems and those found in BLLs with z , is 46. However, according to Zhu & Ménard (2013), Landoni et al. (2013) the expected number of detected Mg II systems in our dataset in the redshift range $0.40 \leq z \leq 1.90$ (with $\text{EW} \geq 1.00\text{\AA}$) should be of the order of ~ 100 . This consideration suggests that, in order to cope with this statistic, the 157 featureless BLLs should lie statistically at redshift $z \lesssim 0.70$ (see also Paiano et al. (2020) for similar conclusions).

5. CONCLUDING REMARKS

We described the ZBLLAC database that currently contains optical spectra for 295 BLLs. We discussed the spectroscopic properties of the objects in this dataset finding that for 35% of them intrinsic spectral features are revealed, allowing to solidly measure the redshift. We reported on 35 targets in which, by detecting intervening absorption systems, we set tight lower limits on their z . On the basis of the absence of absorption lines ascribed to Mg II in 157 featureless object, we statistically suggest that they should lie at low redshift $z \lesssim 0.70$.

The ZBLLAC spectroscopic database of BL Lac objects is an ongoing and still growing project. We encourage other groups to contribute by sharing their own published data. Instructions for joining our

project and contributing to the dataset can be found at <https://web.oapd.inaf.it/zblac/Instructions.pdf>.

6. ACKNOWLEDGEMENTS

We thank B. Sbarufatti (Penn State University, USA), F. Massaro (University of Torino), N. Crespo (ESA), E. Marchesini (Universidad Nacional de La Plata, Buenos Aires), A. Paggi (University of Torino), H. Pena-Herazo (Instituto Nacional de Astrofísica y Electrónica, Mexico), F. Ricci (Pontificia Universidad Católica de Chile), and S. Pita (Université Paris Diderot) for their help in enriching the ZBLLAC database by sharing data.

Source	z	Line	EW Å	FWHM (km/s)	L (erg/s)	Type
ZBLL J0035+5950	0.467	[O II] (λ 3737)	0.3	350	$9.7 \cdot 10^{40}$	N
ZBLL J0050-0929	0.635	[O II] (λ 3727)	0.5	600	$1.0 \cdot 10^{41}$	N
		[O III] (λ 5007)	0.6	450	$9.4 \cdot 10^{40}$	N
		H α (λ 6563)	1.6	1300	$1.6 \cdot 10^{41}$	N
ZBLL J0048+4223	0.302	[O II] (λ 3727)	1.4	920	$4.6 \cdot 10^{40}$	N
		[O III] (λ 5007)	1.2	350	$4.2 \cdot 10^{40}$	N
ZBLL J0158+0101	0.4537	[O III] (λ 5007)	5.0	350	$7.0 \cdot 10^{40}$	N
ZBLL J0303-2407	0.2657	[O III] (λ 5007)	0.2	300	$8.5 \cdot 10^{40}$	N
		H α (λ 6563)	0.2	300	$7.7 \cdot 10^{40}$	N
		[N II] (λ 6585)	0.2	500	$1.0 \cdot 10^{41}$	N
		[O II] (λ 3727)	0.1	450	$1.2 \cdot 10^{41}$	N
ZBLL J0301-1652	0.278	[O III] (λ 5007)	1.5	400	$3.4 \cdot 10^{40}$	N
ZBLL J0305-1608	0.312	[O II] (λ 3727)	2.0	800	$1.7 \cdot 10^{41}$	N
ZBLL J0316-2607	0.443	[O II] (λ 3727)	0.52	1600	$1.3 \cdot 10^{41}$	N
ZBLL J0340-2119	0.223	[O II] (λ 3727)	1.5	1500	$2.9 \cdot 10^{40}$	N
		[O III] (λ 4960)	0.6	1200	$2.6 \cdot 10^{40}$	N
ZBLL J0428-3756	1.105	C III] (λ 1908)	2.3	3500	$6.2 \cdot 10^{42}$	B
		Mg II (λ 2800)	3.0	4500	$6.3 \cdot 10^{42}$	B
		[O II] (λ 3727)	0.5	650	$9.2 \cdot 10^{41}$	N
ZBLL J0509+0542	0.3365	[O II] (λ 3737)	0.07	500	$1.0 \cdot 10^{41}$	N
		[O III] (λ 5007)	0.05	600	$9.2 \cdot 10^{40}$	N
		[N II] (λ 6585)	0.05	300	$6.7 \cdot 10^{40}$	N
ZBLL J0550-3216	0.068	[N II] (λ 6585)	0.8	550	$2.0 \cdot 10^{42}$	N
ZBLL J0757+0956	0.266	[O II] (λ 3727)	0.6	850	$1.4 \cdot 10^{41}$	N
		[O III] (λ 5007)	0.9	1100	$1.9 \cdot 10^{41}$	N
ZBLL J0811+0146	1.148	C III] (λ 1908)	1.0	3000	$2.0 \cdot 10^{42}$	B
		Mg II (λ 2800)	1.5	4000	$3.0 \cdot 10^{42}$	B
ZBLL J0820-1259	0.539	[O II] (λ 3727)	1.2	1000	$5.8 \cdot 10^{41}$	N
		H β (λ 4862)	0.5	850	$1.9 \cdot 10^{41}$	N
		[O III] (λ 5007)	2.5	650	$8.4 \cdot 10^{41}$	N
ZBLL J0930+5132	0.1893	[O III] (λ 4960)	1.0	450	$1.0 \cdot 10^{41}$	N
ZBLL J0942-0047	1.363	C III] (λ 1908)	4.8	200	$4.5 \cdot 10^{41}$	N
		Mg II (λ 2800)	5.0	1600	$1.0 \cdot 10^{43}$	N
ZBLL J1008-3139	0.534	[O II] (λ 3727)	1.0	600	$2.3 \cdot 10^{41}$	N
ZBLL J1012+0631	0.727	Mg II (λ 2800)	0.5	1200	$4.0 \cdot 10^{41}$	N
		[O II] (λ 3727)	0.3	900	$5.0 \cdot 10^{41}$	N
ZBLL J1046+5449	0.252	[O III] (λ 5007)	4.0	700	$1.2 \cdot 10^{41}$	N
ZBLL J1049+1548	0.326	[O II] (λ 3727)	0.3	1200	$1.2 \cdot 10^{41}$	N
ZBLL J1058-8003	0.581	Mg II (λ 2800)	1.2	2500	$4.6 \cdot 10^{42}$	B
		[O III] (λ 4960)	0.5	600	$8.3 \cdot 10^{41}$	N
		[O III] (λ 5007)	1.4	600	$2.5 \cdot 10^{42}$	N
ZBLL J1117+2014	0.140	[O II] (λ 3727)	0.8	1200	$5.2 \cdot 10^{40}$	N
ZBLL J1203-3926	0.227	[O II] (λ 3727)	2.4	600	$6.1 \cdot 10^{40}$	N
		[O III] (λ 4960)	1.4	800	$3.7 \cdot 10^{40}$	N
		[O III] (λ 5007)	2.82	550	$7.3 \cdot 10^{40}$	N
ZBLL J1215+0732	0.137	H α (λ 6563)	1.3	600	$3.3 \cdot 10^{40}$	N
ZBLL J1217+3007	0.129	[O II] (λ 3727)	0.2	600	$6.5 \cdot 10^{40}$	N

		[O III] (λ 5007)	0.2	650	$5.1 \cdot 10^{40}$	N
ZBLL J1221+2813	0.102	[O III] (λ 5007)	0.8	600	$4.8 \cdot 10^{40}$	N
ZBLL J1231+3711	0.219	[O II] (λ 3727)	5.0	1000	$1.4 \cdot 10^{41}$	N
ZBLL J1240+3445	1.636	Mg II (λ 2800)	4.5	3500	$4.2 \cdot 10^{42}$	B
ZBLL J1247+4423	0.569	[O III] (λ 5007)	1.4	400	$1.8 \cdot 10^{41}$	N
ZBLL J1259-2310	0.481	[O II] (λ 3727)	0.9	1100	$4.5 \cdot 10^{41}$	N
		[O III] (λ 5007)	0.4	600	$1.7 \cdot 10^{41}$	N
ZBLL J1309+4305	0.693	[O II] (λ 3727)	1.2	800	$2.0 \cdot 10^{42}$	N
		[O III] (λ 5007)	0.5	600	$5.5 \cdot 10^{41}$	N
ZBLL J1427+2348	0.604	[O II] (λ 3727)	0.1	300	$5.0 \cdot 10^{41}$	N
		[O III] (λ 5007)	0.2	400	$1.1 \cdot 10^{42}$	N
ZBLL J1522-2730	1.297	Mg II (λ 2800)	0.4	2000	$3.0 \cdot 10^{42}$	B
ZBLL J1541+1414	0.223	[O III] (λ 5007)	1.0	500	$3.4 \cdot 10^{40}$	N
ZBLL J1626-7638	0.1050	[O I] (λ 6302)	1.5	1000	$3.7 \cdot 10^{40}$	N
		[S II] (λ 6718 – 6732)	2.0	700	$4.6 \cdot 10^{40}$	N
ZBLL J1637+1314	0.655	[O II] (λ 3727)	0.4	800	$1.5 \cdot 10^{41}$	N
ZBLL J1704+1234	0.452	[O II] (λ 3727)	2.3	900	$4.0 \cdot 10^{41}$	N
		[O III] (λ 4960)	0.7	600	$1.1 \cdot 10^{41}$	N
		[O III] (λ 5007)	3.0	600	$5.0 \cdot 10^{41}$	N
ZBLL J1917-1921	0.137	[O II] (λ 3727)	0.2	600	$3.5 \cdot 10^{40}$	N
		[O III] (λ 4960)	0.2	1000	$2.4 \cdot 10^{40}$	N
		[O III] (λ 5007)	0.5	900	$5.0 \cdot 10^{40}$	N
ZBLL J2009-4849	0.071	H α (λ 6563)	0.3	400	$2.0 \cdot 10^{40}$	N
ZBLL J2134-0153	1.284	C III] (λ 1908)	1.2	1800	$2.2 \cdot 10^{42}$	B
		C II] (λ 2326)	0.5	1800	$9.0 \cdot 10^{41}$	B
		Mg II (λ 2800)	2.3	3500	$4.0 \cdot 10^{42}$	B
ZBLL J2152+1734	0.870	Mg II (λ 2800)	2.7	3000	$1.2 \cdot 10^{42}$	B
		[O II] (λ 3727)	2.2	1100	$9.5 \cdot 10^{41}$	N
ZBLL J2209-0451	0.3967	[O II] (λ 3727)	0.5	300	$7.7 \cdot 10^{40}$	N
ZBLL J2225-1113	0.997	[O II] (λ 3727)	1.8	800	$2.0 \cdot 10^{41}$	N
ZBLL J2246+1544	0.5965	[O II] (λ 3727)	0.9	850	$2.6 \cdot 10^{41}$	N
ZBLL J2250+1749	0.3437	[Ne V] (λ 3426)	1.5	350	$4.3 \cdot 10^{40}$	N
		[O II] (λ 3727)	3.0	500	$9.5 \cdot 10^{40}$	N
		[O III] (λ 4960)	1.0	350	$5.4 \cdot 10^{40}$	N
		[O III] (λ 5007)	4.5	500	$2.3 \cdot 10^{41}$	N
ZBLL J2349+0534	0.419	Mg II (λ 2800)	4.6	3000	$6.6 \cdot 10^{41}$	B
		[O II] (λ 3727)	3.0	1000	$3.5 \cdot 10^{41}$	N
		[O III] (λ 4960)	1.6	750	$1.6 \cdot 10^{41}$	N
		[O III] (λ 5007)	3.5	700	$3.5 \cdot 10^{41}$	N
ZBLL J2357-0152	0.812	Mg II (λ 2800)	1.4	1500	$2.8 \cdot 10^{41}$	N

Table 1. Properties of the emission lines detected in the spectra of BLLs that belong to the ZBLLAC database.

Source	Line	EW (\AA)	z_{abs}
ZBLL J0003+0841	Mg II (λ 2800)	1.50	1.5035
ZBLL J0008+4712	Mg II (λ 2800)	2.00	1.659
ZBLL J0033-1921	Mg II (λ 2800)	0.20	0.505
ZBLL J0038+0012	Mg II (λ 2800)	0.70	0.80

ZBLL J0234–0628	Mg II (λ 2800)	7.00	0.63
ZBLL J0251–1831	Mg II (λ 2800)	3.50	0.615
ZBLL J0338+1302	Mg II (λ 2800)	3.00	0.382
ZBLL J0441–2952	Mg II (λ 2800)	2.15	0.68
ZBLL J0644+6038	Mg II (λ 2800)	5.00	0.581
ZBLL J0649–3139	Mg II (λ 2800)	3.00	0.563
ZBLL J0816–1311	Mg II (λ 2800)	0.15	0.2882
	Mg II (λ 2800)	0.60	0.2336
	Mg II (λ 2800)	1.00	0.1902
ZBLL J0848+7017	Mg II (λ 2800)	11.30	1.2435
ZBLL J1107+0222	Mg II (λ 2800)	2.00	1.0735
ZBLL J1129+3756	Mg II (λ 2800)	9.10	1.211
ZBLL J1231+0138	Ly α (1216)	15.00	3.140
	Mg II (λ 2800)	6.00	2.004
	Fe II (λ 2600)	5.00	2.004
	Mg II (λ 2800)	4.00	2.004
ZBLL J1223+0820	Mg II (λ 2800)	0.90	0.7187
ZBLL J1243+3627	Mg II (λ 2800)	0.90	0.48
ZBLL J1312–2350	Mg II (λ 2800)	2.50	0.462
ZBLL J1351+1114	Mg II (λ 2800)	1.00	0.619
ZBLL J1450+5201	Ly α (λ 1216)	5.80	2.470
	C IV (λ 1908)	3.20	2.470
	C IV (λ 1908)	1.10	2.312
ZBLL J1511–0513	Mg II (λ 2800)	2.10	0.451
ZBLL J1540+8155	Mg II (λ 2800)	0.60	0.672
ZBLL J1730–0352	Mg II (λ 2800)	7.50	0.776
ZBLL J1955–1603	Mg II (λ 2800)	3.00	0.638
ZBLL J1959–4725	Mg II (λ 2800)	2.30	0.519
ZBLL J1200+4009	Ly α (λ 1216)	13.00	3.367
	Mg II (λ 2800)	2.50	1.484
	Fe II (λ 2600)	2.00	1.484
	Mg II (λ 2800)	4.50	1.142
ZBLL J2107–4828	Mg II (λ 2800)	4.30	0.519
ZBLL J2115+1218	Mg II (λ 2800)	4.00	0.497
	Mg II (λ 2800)	0.90	0.525
	Mg II (λ 2800)	0.90	0.633
ZBLL J2139-4235	Ca II ($\lambda\lambda$ 3934-3968)	0.25	0.0087
ZBLL J2212+2759	Mg II (λ 2800)	3.90	1.529
ZBLL J2236–1433	Mg II (λ 2800)	0.70	0.490
	Mg II (λ 2800)	0.90	0.493
ZBLL J2247+0000	Mg II (λ 2800)	3.00	0.898
ZBLL J2255+2410	Mg II (λ 2800)	0.70	0.8633
ZBLL J2319+1612	Mg II (λ 2800)	1.50	0.970
ZBLL J2323+4210	Ca II ($\lambda\lambda$ 3934-3968)	0.50	0.267
	Na I (λ 5892)	0.35	0.267

Table 2. Properties of the intervening absorption lines detected in the spectra of BLL that allow to derive a redshift lower limit.

REFERENCES

- Álvarez Crespo, N., Massaro, F., D'Abrusco, R., et al. 2016a, Ap&SS, 361, 316, doi: [10.1007/s10509-016-2902-1](https://doi.org/10.1007/s10509-016-2902-1)
- Álvarez Crespo, N., Masetti, N., Ricci, F., et al. 2016b, AJ, 151, 32, doi: [10.3847/0004-6256/151/2/32](https://doi.org/10.3847/0004-6256/151/2/32)
- . 2016c, AJ, 151, 32, doi: [10.3847/0004-6256/151/2/32](https://doi.org/10.3847/0004-6256/151/2/32)
- Atwood, W. B., Abdo, A. A., Ackermann, M., et al. 2009, ApJ, 697, 1071, doi: [10.1088/0004-637X/697/2/1071](https://doi.org/10.1088/0004-637X/697/2/1071)
- Blandford, R. D., & Rees, M. J. 1978, in BL Lac Objects, ed. A. M. Wolfe, 328–341
- Bosak, J., & Bray, T. 1999, Scientific American, 280, 89, doi: [10.1038/scientificamerican0599-89](https://doi.org/10.1038/scientificamerican0599-89)
- Costamante, L. 2020, MNRAS, 491, 2771, doi: [10.1093/mnras/stz3018](https://doi.org/10.1093/mnras/stz3018)
- Costamante, L., & Ghisellini, G. 2002, A&A, 384, 56, doi: [10.1051/0004-6361:20011749](https://doi.org/10.1051/0004-6361:20011749)
- D'Abrusco, R., Massaro, F., Paggi, A., et al. 2014, ApJS, 215, 14, doi: [10.1088/0067-0049/215/1/14](https://doi.org/10.1088/0067-0049/215/1/14)
- D'Abrusco, R., Álvarez Crespo, N., Massaro, F., et al. 2019, ApJS, 242, 4, doi: [10.3847/1538-4365/ab16f4](https://doi.org/10.3847/1538-4365/ab16f4)
- de Menezes, R., Peña-Herazo, H. A., Marchesini, E. J., et al. 2019, A&A, 630, A55, doi: [10.1051/0004-6361/201936195](https://doi.org/10.1051/0004-6361/201936195)
- de Menezes, R., Amaya-Almazán, R. A., Marchesini, E. J., et al. 2020, Ap&SS, 365, 12, doi: [10.1007/s10509-020-3727-5](https://doi.org/10.1007/s10509-020-3727-5)
- Falomo, R., Kotilainen, J. K., & Treves, A. 2002, ApJL, 569, L35, doi: [10.1086/340642](https://doi.org/10.1086/340642)
- Falomo, R., Pian, E., & Treves, A. 2014, A&A Rv, 22, 73, doi: [10.1007/s00159-014-0073-z](https://doi.org/10.1007/s00159-014-0073-z)
- Falomo, R., & Treves, A. 1990, PASP, 102, 1120, doi: [10.1086/132740](https://doi.org/10.1086/132740)
- Ghisellini, G., Padovani, P., Celotti, A., & Maraschi, L. 1993, ApJ, 407, 65, doi: [10.1086/172493](https://doi.org/10.1086/172493)
- Landoni, M., Falomo, R., Treves, A., et al. 2013, AJ, 145, 114, doi: [10.1088/0004-6256/145/4/114](https://doi.org/10.1088/0004-6256/145/4/114)
- Landoni, M., Falomo, R., Treves, A., Scarpa, R., & Reverte Payá, D. 2015a, AJ, 150, 181, doi: [10.1088/0004-6256/150/6/181](https://doi.org/10.1088/0004-6256/150/6/181)
- Landoni, M., Paiano, S., Falomo, R., Scarpa, R., & Treves, A. 2018, ApJ, 861, 130, doi: [10.3847/1538-4357/aac77c](https://doi.org/10.3847/1538-4357/aac77c)
- Landoni, M., Massaro, F., Paggi, A., et al. 2015b, AJ, 149, 163, doi: [10.1088/0004-6256/149/5/163](https://doi.org/10.1088/0004-6256/149/5/163)
- Lawrence, C. R., Zucker, J. R., Readhead, A. C. S., et al. 1996, ApJS, 107, 541, doi: [10.1086/192375](https://doi.org/10.1086/192375)
- Maraschi, L., Ghisellini, G., & Celotti, A. 1992, ApJL, 397, L5, doi: [10.1086/186531](https://doi.org/10.1086/186531)
- Marchesi, S., Kaur, A., & Ajello, M. 2018, AJ, 156, 212, doi: [10.3847/1538-3881/aae201](https://doi.org/10.3847/1538-3881/aae201)
- Marchesini, E. J., Peña-Herazo, H. A., Álvarez Crespo, N., et al. 2019, Ap&SS, 364, 5, doi: [10.1007/s10509-018-3490-z](https://doi.org/10.1007/s10509-018-3490-z)
- Massaro, E., Maselli, A., Leto, C., et al. 2015a, Ap&SS, 357, 75, doi: [10.1007/s10509-015-2254-2](https://doi.org/10.1007/s10509-015-2254-2)
- Massaro, F., & D'Abrusco, R. 2016, ApJ, 827, 67, doi: [10.3847/0004-637X/827/1/67](https://doi.org/10.3847/0004-637X/827/1/67)
- Massaro, F., D'Abrusco, R., Ajello, M., Grindlay, J. E., & Smith, H. A. 2011, ApJL, 740, L48, doi: [10.1088/2041-8205/740/2/L48](https://doi.org/10.1088/2041-8205/740/2/L48)
- Massaro, F., D'Abrusco, R., Paggi, A., et al. 2013, ApJS, 206, 13, doi: [10.1088/0067-0049/206/2/13](https://doi.org/10.1088/0067-0049/206/2/13)
- Massaro, F., D'Abrusco, R., Tosti, G., et al. 2012a, ApJ, 750, 138, doi: [10.1088/0004-637X/750/2/138](https://doi.org/10.1088/0004-637X/750/2/138)
- . 2012b, ApJ, 752, 61, doi: [10.1088/0004-637X/752/1/61](https://doi.org/10.1088/0004-637X/752/1/61)
- Massaro, F., Landoni, M., D'Abrusco, R., et al. 2015b, A&A, 575, A124, doi: [10.1051/0004-6361/201425119](https://doi.org/10.1051/0004-6361/201425119)
- Massaro, F., Masetti, N., D'Abrusco, R., Paggi, A., & Funk, S. 2014, AJ, 148, 66, doi: [10.1088/0004-6256/148/4/66](https://doi.org/10.1088/0004-6256/148/4/66)
- Massaro, F., D'Abrusco, R., Landoni, M., et al. 2015c, ApJS, 217, 2, doi: [10.1088/0067-0049/217/1/2](https://doi.org/10.1088/0067-0049/217/1/2)
- Massaro, F., Álvarez Crespo, N., D'Abrusco, R., et al. 2016, Ap&SS, 361, 337, doi: [10.1007/s10509-016-2926-6](https://doi.org/10.1007/s10509-016-2926-6)
- Miller, J. S., French, H. B., & Hawley, S. A. 1978, in BL Lac Objects, ed. A. M. Wolfe, 176–187
- Nori, M., Giroletti, M., Massaro, F., et al. 2014, ApJS, 212, 3, doi: [10.1088/0067-0049/212/1/3](https://doi.org/10.1088/0067-0049/212/1/3)
- Padovani, P., & Giommi, P. 1995a, MNRAS, 277, 1477, doi: [10.1093/mnras/277.4.1477](https://doi.org/10.1093/mnras/277.4.1477)
- . 1995b, ApJ, 444, 567, doi: [10.1086/175631](https://doi.org/10.1086/175631)
- Paggi, A., Milisavljevic, D., Masetti, N., et al. 2014, AJ, 147, 112, doi: [10.1088/0004-6256/147/5/112](https://doi.org/10.1088/0004-6256/147/5/112)
- Paiano, S., Falomo, R., Treves, A., Franceschini, A., & Scarpa, R. 2019, ApJ, 871, 162, doi: [10.3847/1538-4357/aaf6e4](https://doi.org/10.3847/1538-4357/aaf6e4)
- Paiano, S., Falomo, R., Treves, A., & Scarpa, R. 2018, ApJL, 854, L32, doi: [10.3847/2041-8213/aaad5e](https://doi.org/10.3847/2041-8213/aaad5e)
- . 2020, MNRAS, 497, 94, doi: [10.1093/mnras/staa1840](https://doi.org/10.1093/mnras/staa1840)
- Paiano, S., Franceschini, A., & Stamerra, A. 2017a, MNRAS, 468, 4902, doi: [10.1093/mnras/stx749](https://doi.org/10.1093/mnras/stx749)
- Paiano, S., Landoni, M., Falomo, R., Treves, A., & Scarpa, R. 2017b, ApJ, 844, 120, doi: [10.3847/1538-4357/aa7aac](https://doi.org/10.3847/1538-4357/aa7aac)
- Paiano, S., Landoni, M., Falomo, R., et al. 2017c, ApJ, 837, 144, doi: [10.3847/1538-4357/837/2/144](https://doi.org/10.3847/1538-4357/837/2/144)
- Peña-Herazo, H. A., Marchesini, E. J., Álvarez Crespo, N., et al. 2017, Ap&SS, 362, 228, doi: [10.1007/s10509-017-3208-7](https://doi.org/10.1007/s10509-017-3208-7)
- Peña-Herazo, H. A., Massaro, F., Chavushyan, V., et al. 2019, Ap&SS, 364, 85, doi: [10.1007/s10509-019-3574-4](https://doi.org/10.1007/s10509-019-3574-4)

- Pita, S., Goldoni, P., Boisson, C., et al. 2014, *A&A*, 565, A12, doi: [10.1051/0004-6361/201323071](https://doi.org/10.1051/0004-6361/201323071)
- Plotkin, R. M., Anderson, S. F., Brandt, W. N., et al. 2010, *AJ*, 139, 390, doi: [10.1088/0004-6256/139/2/390](https://doi.org/10.1088/0004-6256/139/2/390)
- Ricci, F., Massaro, F., Landoni, M., et al. 2015, *AJ*, 149, 160, doi: [10.1088/0004-6256/149/5/160](https://doi.org/10.1088/0004-6256/149/5/160)
- Sandrinelli, A., Treves, A., Falomo, R., et al. 2013, *AJ*, 146, 163, doi: [10.1088/0004-6256/146/6/163](https://doi.org/10.1088/0004-6256/146/6/163)
- Sbarufatti, B., Ciprini, S., Kotilainen, J., et al. 2009, *AJ*, 137, 337, doi: [10.1088/0004-6256/137/1/337](https://doi.org/10.1088/0004-6256/137/1/337)
- Sbarufatti, B., Falomo, R., Treves, A., & Kotilainen, J. 2006, *A&A*, 457, 35, doi: [10.1051/0004-6361:20065455](https://doi.org/10.1051/0004-6361:20065455)
- Sbarufatti, B., Treves, A., & Falomo, R. 2005a, *ApJ*, 635, 173, doi: [10.1086/497022](https://doi.org/10.1086/497022)
- Sbarufatti, B., Treves, A., Falomo, R., et al. 2005b, *AJ*, 129, 559, doi: [10.1086/427138](https://doi.org/10.1086/427138)
- Shakura, N. I., & Sunyaev, R. A. 1973, *A&A*, 500, 33
- Shaw, M. S., Romani, R. W., Cotter, G., et al. 2013, *ApJ*, 764, 135, doi: [10.1088/0004-637X/764/2/135](https://doi.org/10.1088/0004-637X/764/2/135)
- Shen, Y., Richards, G. T., Strauss, M. A., et al. 2011, *ApJS*, 194, 45, doi: [10.1088/0067-0049/194/2/45](https://doi.org/10.1088/0067-0049/194/2/45)
- Stickel, M., Fried, J. W., & Kuehr, H. 1988, *A&A*, 191, L16 —. 1989, *A&AS*, 80, 103
- Stickel, M., Padovani, P., Urry, C. M., Fried, J. W., & Kuehr, H. 1991, *ApJ*, 374, 431, doi: [10.1086/170133](https://doi.org/10.1086/170133)
- Stocke, J. T., Liebert, J., Schmidt, G., et al. 1985, *ApJ*, 298, 619, doi: [10.1086/163646](https://doi.org/10.1086/163646)
- Urry, C. M., & Padovani, P. 1995, *PASP*, 107, 803, doi: [10.1086/133630](https://doi.org/10.1086/133630)
- Vernet, J., Dekker, H., D'Odorico, S., et al. 2011, *A&A*, 536, A105, doi: [10.1051/0004-6361/201117752](https://doi.org/10.1051/0004-6361/201117752)
- Wakely, S. P., & Horan, D. 2008, in International Cosmic Ray Conference, Vol. 3, International Cosmic Ray Conference, 1341–1344
- Zhu, G., & Ménard, B. 2013, *ApJ*, 770, 130, doi: [10.1088/0004-637X/770/2/130](https://doi.org/10.1088/0004-637X/770/2/130)